academicJournals

Vol. 7(1), pp. 10-21, January 2015
DOI: 10.5897/JETR2014.0520
Article Number:E195CAA49702
ISSN 2006-9790

http://www.academicjournals.org/JETR

Journal of Engineering and Technology Research

*Full Length Research Paper*

# Effect of oxygen plasma treatments on the structural and optical properties of polyimide films

**A. Atta* and S. M. El-Sayed**

Department of Physics, National Center for Radiation Research and Technology, Nasr City, Cairo, Egypt.

Received 30 September, 2014; Accepted 17 December, 2014

**A detailed study of some physical properties of Polyimide films after exposing them to oxygen plasma is presented. The structure of the sample has been analyzed by X-ray diffraction technique (XRD) and is found to be semi crystalline. Thermogravimetric Analysis (TGA) studies revealed that the thermal stability of polyimide films have improved after being exposed to oxygen plasma, at different time intervals, ranging from 1 to 5 min. Optical constants such as refractive index (n), extinction coefficient (K) and complex dielectric constant have been determined. A great dependence of the fundamental optical constants on the exposure time was noticed. Upon exposure to oxygen plasma, decrease in the refractive index was obtained. On the other hand the driving absorption coefficient (α) and consequently the optical band gap have been estimated. The real (ε`) and imaginary parts (ε``) of the dielectric constant have been determined. The dispersion parameters such as $E_0$ (single-oscillator energy), $E_d$ (dispersive energy) and $M_{-1}$, $M_{-3}$ (moments) were calculated and discussed.**

**Key words:** Plasma deposition, X-ray diffraction (XRD), crystal structure, optical properties, thermogravimetric analysis (TGA).

## INTRODUCTION

Polymer-based optical materials are particularly attractive in integrated optical waveguide devices because they can offer rapid processibility, cost-effectiveness, high yields, and high performance, such as smaller birefringence compared to silica. Furthermore, optical polymers provide an ideal platform for incorporation of more complex material functionalities through different doping or reaction agents, thereby enabling amplification and electro-optic effects to be achieved, once the passive optical polymer technology is established (Ma et al., 2002). Conventional optical polymers, such as polymethylmethacrylate (Kagami et al., 1995), polystyrene (Gokan et al., 1982) and polycarbonate (Singh et al., 1996) possess different structures and demonstrate many attractive properties, but not all of them possess the needed thermal stability for direct on-chip interconnect applications.

Polyimide has found widespread applications in industry for insulation of electrical machines (Verdianz et al., 2006) as optical materials, for flexible print circuits (Choi et al., 2009). Polyimide based materials have also been applied as electrodes in biomedical micro-devices (Mercanzini et al., 2009).

In this regard, polyamides are a proven class

*Corresponding author. E-mail: alyatta2001@yahoo.com, Tel: 02-22875924. Fax: (00202)22876031.

of polymers in the microelectronics industry due to their outstanding properties, especially for their high thermal stability. Polyimides (PIs) are a class of representative high performance polymers possessing the cyclic imide and aromatic groups in the main chains. At present, Polyimides (PIs) are extensively used in the microelectronics, photonics, optics, and aerospace industries not only for their very excellent thermal stability but also for their good mechanical properties, low dielectric constant, low coefficient of thermal expansion, and high radiation resistance. Significant effort has been expended to improve their properties further by modification of the chain backbones and higher-order structure control (Atta, 2013; Hasegawa and Horie, 2001). Due to its easy synthesis and attractive optical properties, polyimide is expected to play an important role in the field of organic optical waveguides.

Plasmas generated are widely used to activate polyimide properties. The properties are characterized by the modification of chemical and physical properties which is based on chain scission, the formation of functional groups, and cross-linking (Atta et al., 2014). The energetic electrons, ions, excited atoms, molecules, and UV photons present in the gas phase are responsible for the material modification, but their role in the interaction with the polymer is yet not fully understood due to the complexity of the gas phase and the polymer structure (Hasegawa and Horie, 2001). The polymer films are bombarded by the plasma active species mentioned above just described that leads to chain scissions and polymer degradation. If a plasma reactive gas is used, the appearance of new functional groups on the film will be expected. The most important feature of the plasma technique is the ability to control the modification of the polymer properties. Reactions between plasma species and polymer film make it possible to form polar groups on the film for instance C-O, C=O, O-C=O are chemically reactive and cause an increase of the surface energy and wetting qualities (Atta et al., 2013). Here, the intention of this study is to investigate the effect of oxygen exposure time on the polyimide films has been carried out using X-ray Diffraction (XRD), Thermogravimetric Analysis (TGA) and optical properties.

## EXPERIMENTAL

Polyimide (Kapton) films of thickness 160 μm (Du Pont, USA) were used for oxygen plasma exposure process. We use the reactive ion etching (RIE) technique system with the following Oxygen plasma parameters, the working pressure is $7.3E^{-3}$ mBar; Oxygen gas flow rate is 25 s/cm; and the incident power is kept constant at 100 W, with a corresponding DC self-bias voltage – 275 V and the exposure time varied from 0 to 5 min. The exposure process was performed using a Radio-Frequency (RF) of 13.56 MHZ at National Laboratory of Advanced Technology and Nano-Science (INFM-TASC), Trieste, Italy. Before performing the plasma treatment, the polyimide polymeric samples were first cleaned by acetone using ultrasonic technique in order to remove contamination on the polymeric surface. XRD scanning was carried out using fully computerized X-ray diffractometer (Shimadzu type XD-DI). Filtered copper radiation, $\lambda$*=1.542A* was used in this investigation. The X-ray tube was operated at *40 kV* and *30 mA* anode current throughout the measurements. The pattern was recorded at a scanning rate of 4°*/min*. The above operation conditions were maintained during all the relevant measurements. Hence, it is a plot of the intensity against the angle *2*$\theta$, where $\theta$ is the reflection angle of X-ray given in Bragg's equation $2d\sin\theta = n\lambda$. The thermal stability of the polyimide films was investigated by Thermo Gravimetric Analysis (TGA) (Shimadzu, Japan). The TGA measurements were carried out in $N_2$ atmosphere from room temperature to 500°C using a heating rate of 10°C/min.

Optical density of absorbance for the deposited and exposure films was measured over range of 200 to 2500 nm using Kontron – UV/VIS spectrophotometer (made in Switzerland). Different parts along the entire film were measured until good reproducibility of the respective absorption and transmission spectra was achieved. The obtained absorption data against incident light wavelength were used to calculate the electronic absorption coefficient ($\alpha$ $cm^{-1}$) and hence the optical energy gap as well as the volume and surface energy loss functions.

## RESULTS AND DISCUSSION

### Oxygen plasma exposure effects on X-ray diffraction studies

The X-ray diffraction scans of ¨Polyimide films as a function of Bragg angle (2θ) are displayed in Figure 1 for virgin and all oxygen plasma exposure time. The diffraction pattern of virgin polymer clearly indicates that this polymer is semi-crystalline in nature. The X-ray diffraction data of the virgin sample (Table 1) shows three peaks at 2$\theta$= 14.88°, 21.78° and 26.255° with lattice spacing *d* = 5.94882Å, 4.0773Å and 3.39162Å, and the corresponding full widths at half maxima (FWHM) are 2.84°, 3.08° and 2.23°, respectively. The diffraction pattern of virgin sample showed partial crystallinity and the most intense peak appeared at 2θ= 26.255°. However, in case of increasing the plasma exposure, a significant change in the diffraction pattern has been observed (Table 1). The diffraction patterns of the virgin sample and exposed samples at different time are quite different and the three original peaks are found at slightly higher angular positions respectively. It is evident that the diffraction pattern of the exposure Polyimide is broader than the virgin one, which indicates a decrease in crystallinity. Similar finding was represented in (Qi et al. 2006 and Shalaby et al. 2013).

As shown in Table 2 by increasing the time of exposure to the oxygen plasma, there is always a possibility of development of strain (stress), which affects the mechanical properties of the samples such as the stability of microstructure, the strain (stress) in a sample can be intrinsic, caused by the conditions prevailing during deposition. On other hand, strain (stress) can be extrinsic to the sample but intrinsic to the composite – substrate system, caused by the difference in thermal expansion coefficient (Bin Ahmed et al., 2012). The

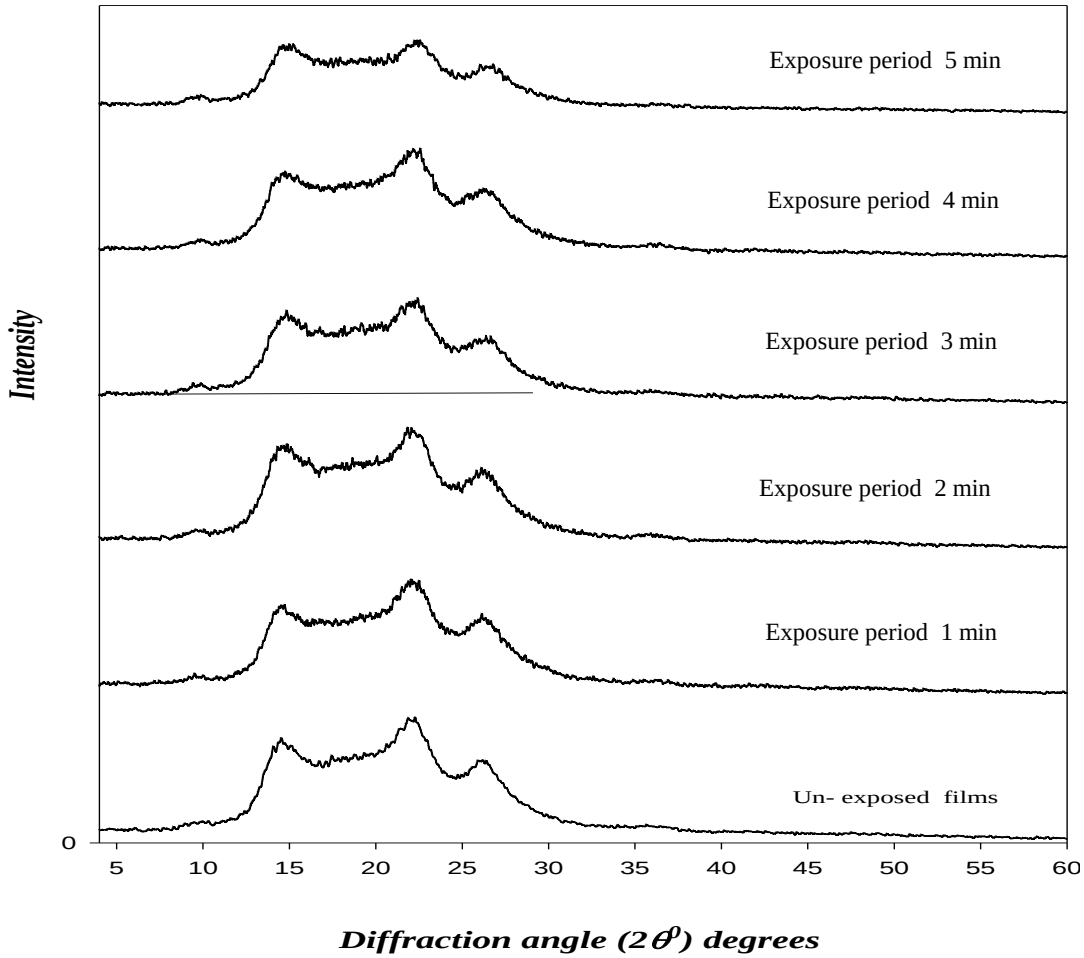


**Figure 1.** X- ray diffraction patterns spectra for polyimide film with oxygen plasma exposure time.

**Table 1.** The X-ray diffraction data for PI as a function of plasma exposure time.

| Films | First Peak | | | Second Peak | | | Third Peak | | |
|---|---|---|---|---|---|---|---|---|---|
| | d (A) | 2ϑ | FWHM | d (A) | 2ϑ | FWHM | d (A) | 2ϑ | FWHM |
| Virgin Film | 4.077 | 21.780 | 3.08 | 5.949 | 14.88 | 2.84 | 3.395 | 26.290 | 2.88 |
| Exposed 1 min | 4.065 | 21.846 | 2.93 | 6.021 | 14.70 | 2.29 | 3.392 | 26.270 | 2.26 |
| Exposed 2 min | 4.056 | 21.543 | 2.92 | 6.062 | 14.60 | 2.14 | 3.390 | 26.255 | 2.50 |
| Exposed 3 min | 4.001 | 22.340 | 2.82 | 6.106 | 14.53 | 2.11 | 3.387 | 26.243 | 2.22 |
| Exposed 4 min | 3.813 | 22.200 | 2.32 | 6.155 | 14.38 | 2.04 | 3.351 | 26.230 | 2.23 |
| Exposed 5min | 3.781 | 22.109 | 2.28 | 6.197 | 14.26 | 1.56 | 3.317 | 26.060 | 1.96 |

crystallite size and the residual strain are calculated from full width at half maximum (FWHM) using the relation (1) for all phases

$$P = \frac{K\lambda}{\beta\cos\theta} \quad \beta = \frac{\lambda}{D\cos\theta} - \varepsilon\tan\theta \quad \delta = \frac{1}{D^2} \qquad (1)$$

where ($\beta$) is full width at half maxima (FWHM) in radians, the wavelength, $\lambda$ of X-ray beam (1×5418 Å), *P* the crystallite size in A° and *K is* a constant for most cases it is close to 1. Assuming *K* = 1 in Equation (1), the crystallite sizes were calculated for strong peaks in all samples as given in Table 2. However, particularly in case of solid polymeric materials, the exact nature of the interrelation between spacing, crystallite size and the

**Table 2.** The crystallite size for PI as a function of plasma exposure time.

| Films | First Peak | | | Second Peak | | | Third Peak | | |
|---|---|---|---|---|---|---|---|---|---|
| | P(m) E-09 | δ E-16 | Δ (ε) E-2 | P(m) E-09 | δ | Δ (ε) E-2 | P(m) E-09 | δ | Δ (ε) E-2 |
| Virgin Film | 2.746 | 13.267 | 1.783 | 2.949 | 11.501 | 2.423 | 2.961 | 11.407 | 1.374 |
| Exposed 1 min | 2.884 | 12.030 | 1.693 | 3.651 | 7.500 | 1.980 | 3.773 | 7.025 | 1.194 |
| Exposed 2 min | 2.883 | 12.021 | 1.717 | 3.912 | 6.534 | 1.861 | 3.412 | 8.597 | 1.079 |
| Exposed 3 min | 3.002 | 11.100 | 1.591 | 3.973 | 6.335 | 1.841 | 3.841 | 6.779 | 1.066 |
| Exposed 4 min | 3.647 | 7.517 | 1.318 | 4.103 | 5.941 | 1.802 | 3.823 | 6.841 | 1.061 |
| Exposed 5min | 3.711 | 7.262 | 1.300 | 5.365 | 3.457 | 1.389 | 4.349 | 5.288 | 0.944 |

**Table 3.** The interchain distance (r), interplaner distance (d) and the distortion parameter (g) for PI as a function of plasma exposure time.

| Films | First Peak | | | Second Peak | | | Third Peak | | |
|---|---|---|---|---|---|---|---|---|---|
| | *r* E-10 | *d* E-10 | *g* E-10 | *r* E-10 | *d* E-10 | *g* E-10 | *r* E-10 | *d* E-10 | *g* E-10 |
| Virgin Film | 5.101 | 4.081 | 0.279 | 7.442 | 5.954 | 0.38 | 4.237 | 3.390 | 0.215 |
| Exposed 1 min | 5.085 | 4.068 | 0.265 | 7.532 | 6.026 | 0.310 | 4.240 | 3.392 | 0.169 |
| Exposed 2 min | 5.156 | 4.124 | 0.269 | 7.584 | 6.067 | 0.292 | 4.243 | 3.394 | 0.187 |
| Exposed 3 min | 4.974 | 3.979 | 0.249 | 7.620 | 6.096 | 0.288 | 4.245 | 3.396 | 0.166 |
| Exposed 4 min | 5.005 | 4.004 | 0.206 | 7.699 | 6.159 | 0.282 | 4.247 | 3.397 | 0.167 |
| Exposed 5 min | 5.026 | 4.021 | 0.204 | 7.764 | 6.211 | 0.218 | 4.274 | 3.419 | 0.148 |

degree of disorder is yet to be understood in proper perspective. These bands agree with those elsewhere reported (Liu et al., 2002; Sahaet al., 2009)

The strain *(ε)* was calculated from the slope of the *(βcosθ)* versus (*sinθ*) plot using the Equation (1). The dislocation density *(δ),* defined as the length of dislocation lines per unit volume of the crystal, was evaluated from the Equation 1. Table 3 showed that the decrease in X-ray intensity may be resulting from grain size. This appears as boarding beaks, on the other hand, decreasing in the interchain distance (r) and the interplaner distance in the peaks lead to deceasing in crystallinty.

$$r = \frac{5\lambda}{8\sin\theta} \qquad d = \frac{\lambda}{2\sin\vartheta} \qquad g = \frac{\beta}{\tan\theta} \tag{2}$$

Where interchain distance (r) and d is interplaner distance. Also, g is distortion parameter. From Table 2 it has been observed that the crystallite size decreases but strain and dislocation density in the samples increase with the increase in the time of exposure by oxygen. However, the decrease in intensity and the shift in angular position towards the higher angle can be explained by the decrease in lattice spacing (*r* and *d*). It also suggests a change in crystallite size of the samples exposed to oxygen plasma at different times. The crystallite sizes of the virgin and irradiated Polyimide-polymer have been calculated using Scherrer's equation (Equation 1).

**Thermogravimetric analysis (TGA)**

Oxygen plasma exposure effects on the thermal stability of polymer were evaluated by TGA. TGA is a technique used to accurately track the *in situ* weight changes of a sample during the heating process, thereby providing information on thermal degradation. Figure 2a, b shows the TGA curves for deposited films and also exposed film at period 5 min. From Figure 2a, b, it is evident that the thermal oxidative degradation of the samples involved two different steps in the whole process. This is probably because the first step at 300°C (about 1.5% weight loss in TGA curve at this temperature) resulted in some decomposition and consequently hindered the crystallization of polyimide on the second step. It is clear that this polyimide exhibited excellent thermal stability, since no obvious weight loss was found in the differential thermogravimetric (TGA) curve below 500°C. This indicated that crystallization of the polyimide occurred rapidly during the thermal imidization of precursor, and semicrystalline polyimide can be readily obtained. The increase in the weight residues above 500°C illustrates successful incorporation of higher exposure period time (5 min of oxygen plasma) as shown in Figure 2b, and ultimately increases in thermal stability. The improvement of the thermal stability of the polyimide by increasing plasma exposure can be based on the fact that these

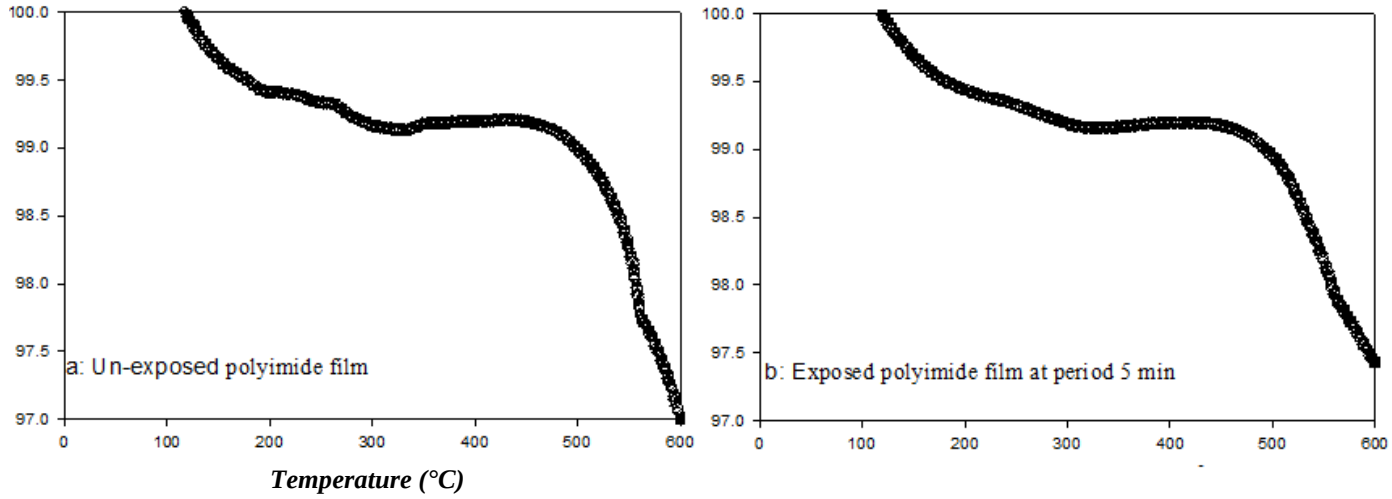


**Figure 2.** TGA curves for a-unexposed and b-exposed polyimide film with 5 min oxygen plasma.

materials have inherently good thermal stability and also due to the strong interaction/chemical bonding that exposed the polyimide film. These results suggest that molecules are bonding to the polyimide through reaction with H bonds and possibly through functionalities resulting from oxidative degradation of the polyimide film. The difference is mainly attributable to the different responses of the polymers to the evolution systems. One of the most important key parameters is the *T*GA of the optical device fabrication.

## UV-Visible spectrophotometric measurements

Figure 3 shows the transmittance spectra, obtained at room temperature and near normal incidence for virgin film and different oxygen plasma exposure (1, 2, 3, 4 and 5 min) in the visible region. As can be seen from this Figure 3, the obtained films are characterized with high transmission greater than 60% for 600 nm depending on the film exposed by oxygen.

The transmittance decreases as the exposure time increases at wavelength λ = 600 nm and it can be positively concluded that the material is of highly absorbing nature. The absorption coefficient was calculated from transmittance measurements with the aid of the expression (Kiryong and John, 2002).

$$\alpha = \frac{2.303}{d}\log_{10}\left(\frac{1}{T}\right) \quad (3)$$

where d is the thickness of the film and T is the transmittance. If the sample faces are parallel, which is in most of the current case, multiple reflections have to be taken into account within the sample thickness. In this work, the polymer films are sufficiently thick compared to the beam wavelength to neglect the interference phenomena. The air/polymer interface transmission T is expressed as functions of refractive index (n) and extinction coefficient (K) (Soldera et al., 200).

$$T = \frac{4n}{(n+1)^2 + k^2} \quad (4)$$

Once the measurements of value T is done, an iterative procedure to calculate n and K is initiated. When the absorption $\alpha$ is known, the extinction coefficient K can be found the relation $K = \alpha\lambda/4\pi$ . It is found that the value of n decreases, while the value of K increases with the photon energy at different time exposure. Oxygen plasma exposure has effect on the spectral dependence of (n) on wavelength λ for films as shown in Figure 4. The high-frequency properties for virgin film and films exposure by oxygen plasma could be treated by using Cauch's formula (Jenkins et al., 1985). It was found that the high-frequency dielectric constant $\varepsilon_\infty$ can be determined from the plots of $(n^2 - 1)^{-1}$ versus $\lambda^{-2}$ as shown in Figure 5.

The Cauch's formula describes the contribution of free carriers and lattice modes. To obtain information about direct or indirect transitions, the optical band gap was determinate from analysis of the spectral dependence of the absorption near the fundamental absorption within the framework of an electron theory (Kumar et al., 2000). Thus, the electronic transition between valance and conduction band is given by

$$\alpha h\nu = A(h\nu - E_g)^s \quad (5)$$

Where s has discrete values like 1/2, 3/2, 2 or more

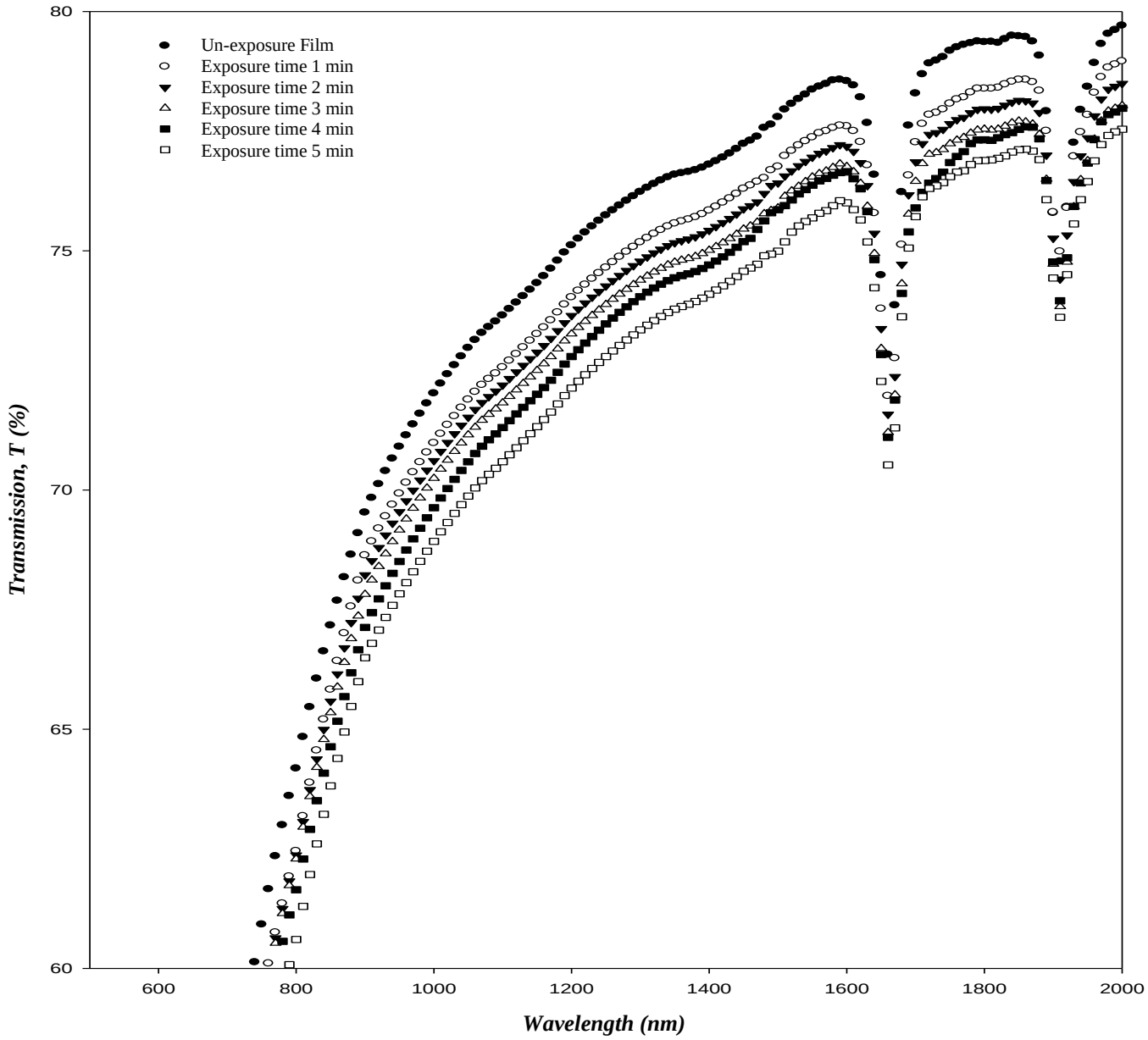


**Figure 3.** Transmission spectra for polyimide film with oxygen plasma exposure time.

depending on whether the transition is direct or indirect and allowed or forbidden. In the equation 5, A is constant, h is Plank's constant, $E_g$ the optical band gap and $h\nu$ the energy photon. Plotting $(\alpha h\nu)^{1/2}$ as a function of the photon energy $h\nu$ for the curves (un-exposed and exposed films) is shown in Figure 6. This liner region characterizes an optical gap $E_g$ according to Equation 5. The linear region in Figure 6 is used to obtain the values of optical band gaps (namely $E_g$). The values of $E_g$ for all studied films are calculated and listed in Table 4. It is clear that the Polyimide film with thickness (0.160 mm) shows an energy gap $E_g$. And also, all films revealed an additional energy gap $E_g$ at higher wavelength due to the decreased grain size of the higher time exposure films and also results in the decrease in crystalline nature which in turns decrease the band gap. Where, the peaks in UV-Vis region have generally interpreted in terms of $\pi \rightarrow \pi^*$ transition between bonding and antibonding molecular orbital. Assuming that the frequency is relatively, the real part ε`and imaginary part ε``. Parts of the complex dielectric constant can be written according

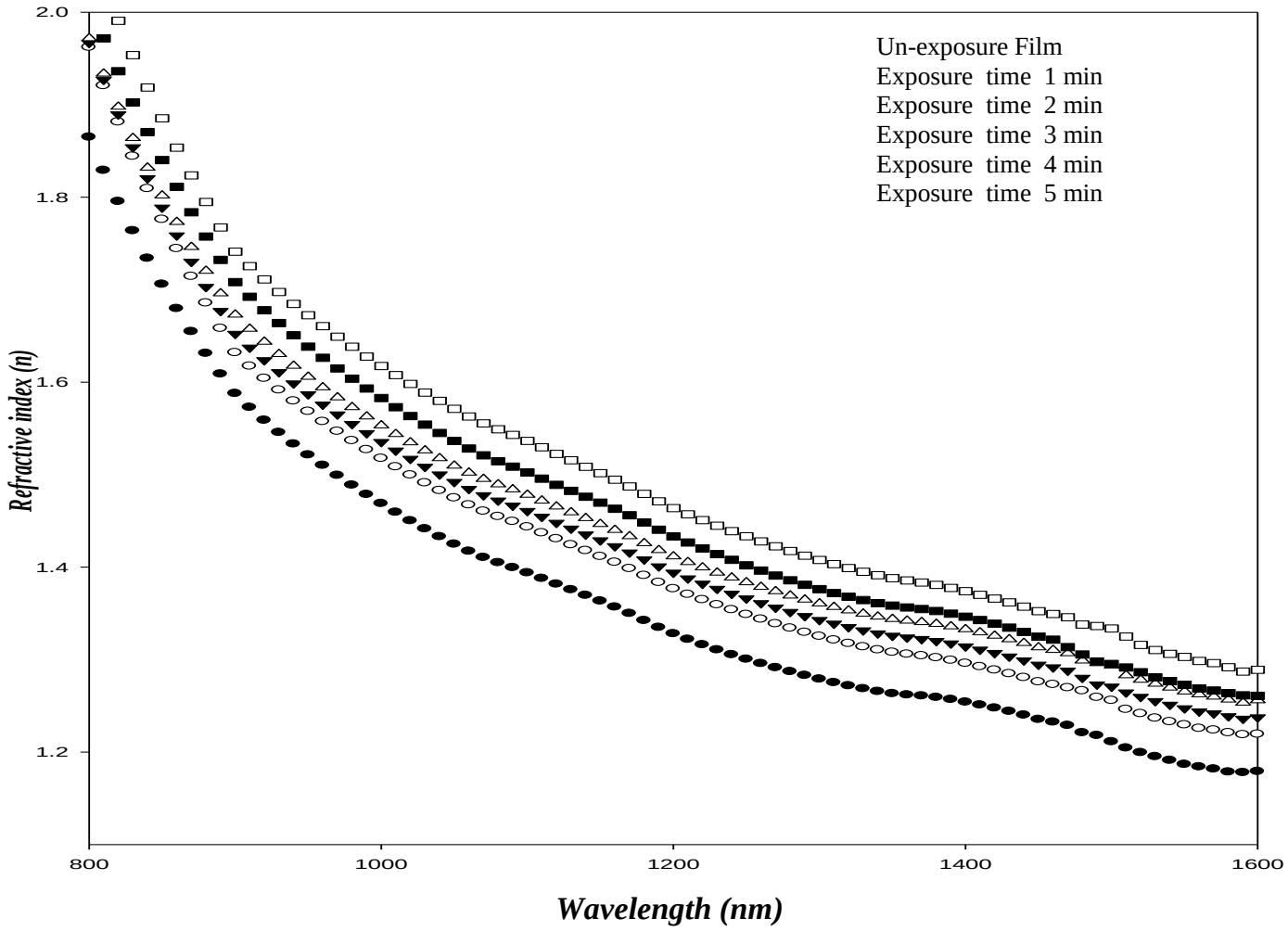


**Figure 4.** Wavelength dependence of the refractive index *n* with oxygen plasma exposure time for polyimide film.

to the following relations (Wakkad et al., 2000).

$$\varepsilon` = n^2 - K^2 = \varepsilon_\infty - \frac{e^2}{4\pi^2 C^2 \varepsilon_0} \frac{N}{m^*} \lambda^2 \quad (6)$$

and

$$\varepsilon`` = 2nK = \frac{\varepsilon_\infty \omega_p^2}{8\pi^2 C^3 \tau} \lambda^3 \quad (7)$$

where

$$\omega_p = \left[ \frac{e^2 N}{\varepsilon_0 \varepsilon_\infty m^*} \right]^{1/2} \quad (8)$$

Where $\omega_P$ is the plasma resonance frequency for one kind of the free carriers, $\varepsilon_\infty$ is the high frequency dielectric constant, e is the electronic charge, C is the velocity of light, $\varepsilon_o$ is the free space dielectric constant, N /m* is the ratio of free carrier concentration (N) to the free carrier effective mass (m*) and $\tau$ is the optical relaxation time.

Equations (6) to (8) were employed to determine the parameters $\varepsilon_\infty$ ,$\omega_p$ and N/m*. The values $\omega_p$ and N/m* decreased by increasing oxygen plasma exposure time from 1 up to 5 min as shown in Figure 7. On the other hand, the shift of plasma edge towards higher frequency in the present case could be attributed to the relatively higher value of carrier concentration as mentioned before. This could be accounted for by the generation of excess electronic delocalized states.

The refractive index and the single oscillator parameters were calculated and discussed in terms of the Wemple-DiDmenico model (Wemple, 1973). That the parameters $E_o$, $E_d$ are calculated by know oscillator energy $E_o$ which is independent of the scale of $\varepsilon$ and is consequently an “average” energy gap, where as $E_d$ depends on the scale of $\varepsilon$ and thus serves as an

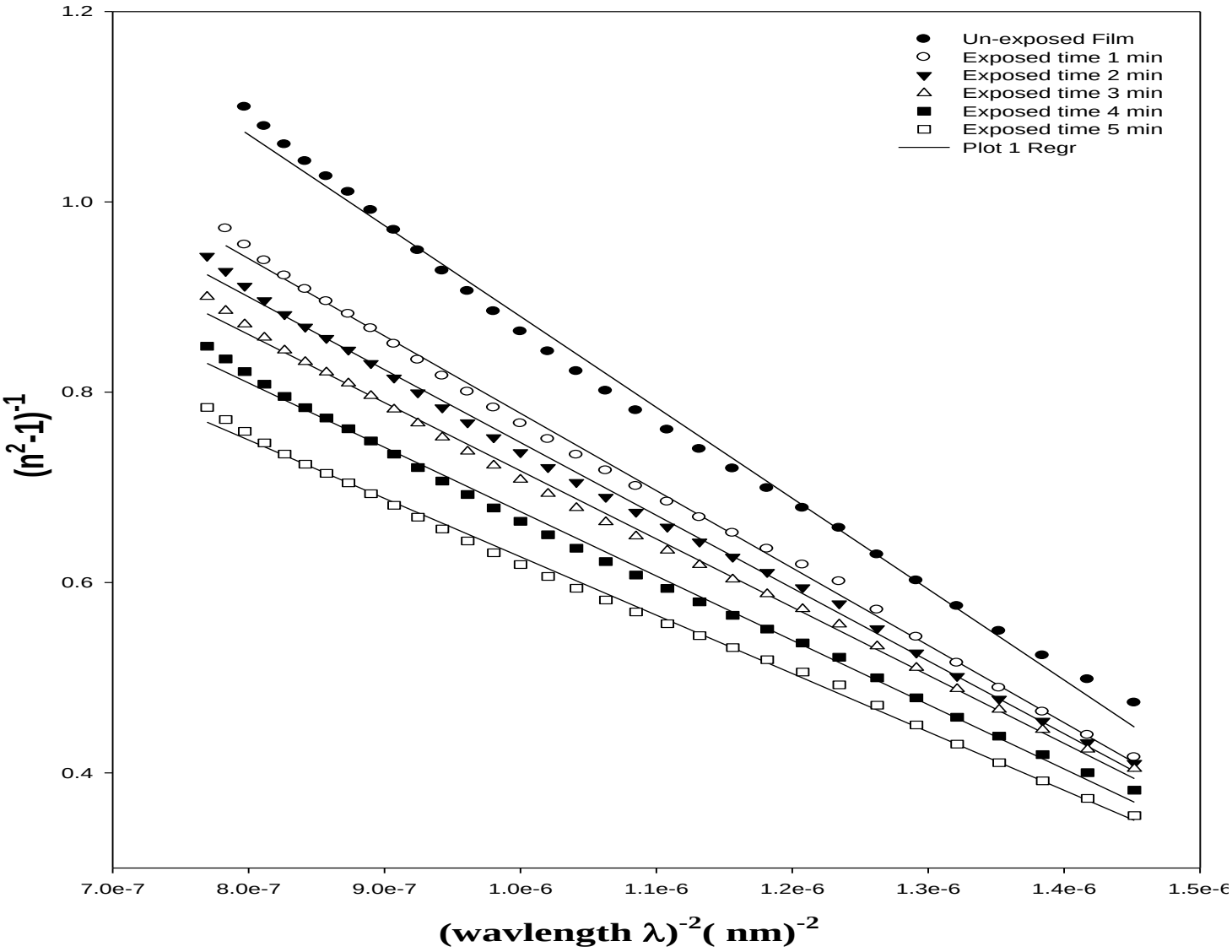


**Figure 5.** Plots $(n^2 - 1)^{-1}$ against square wavelength ($\lambda^{-2}$) with oxygen plasma exposure time for polyimide film.

interband strength parameters. Since the $M_o$ and $M_d$ moments are involved most heavily near the interband absorption edge.

The dispersion of refractive index below the interband absorption edge has been obtained according to the single oscillator model (Wemple, 1973; Wemple and Didomenico, 1971).

$$n^2(E) = 1 + \left[ \frac{E_0 E_d}{E_0^2 - E^2} \right] \quad (9)$$

where the parameters $E_o$, $E_d$ are the single-oscillator energy and dispersive energy respectively. By plotting $(n^2 - 1)^{-1}$ versus $E^2$ and fitting a straight line as shown in Figure 8, $E_o$ and $E_d$ are determined directly from the gradient, $(E_o , E_d )^{-1}$ and the intercept $(E_o / E_d )$, on the vertical axis. Therefore, in order to account for the trend of $E_d$, it is suggested that the observed increase in $E_d$ is with increasing exposed time is primarily a crosslinking. It is shown that a peculiarity for $E_o$, $E_d$. On the basis of the above-mentioned model the single–oscillator parameters $E_o$, $E_d$ are related to the imaginary part, $\varepsilon``$ of the complex dielectric constant, the $M_{-1}$, $M_{-3}$ moments of polyimide can be derived from the relations (Yakuphanoglu et al., 2004)

$$E_0^2 = \frac{M_{-1}}{M_{-3}} \text{ and } E_d^2 = \frac{M_{-1}^3}{M_d} \quad (10)$$

So that the higher energy interband transitions that influence $M_{-1}$ have little influence on $E_d$. However, within

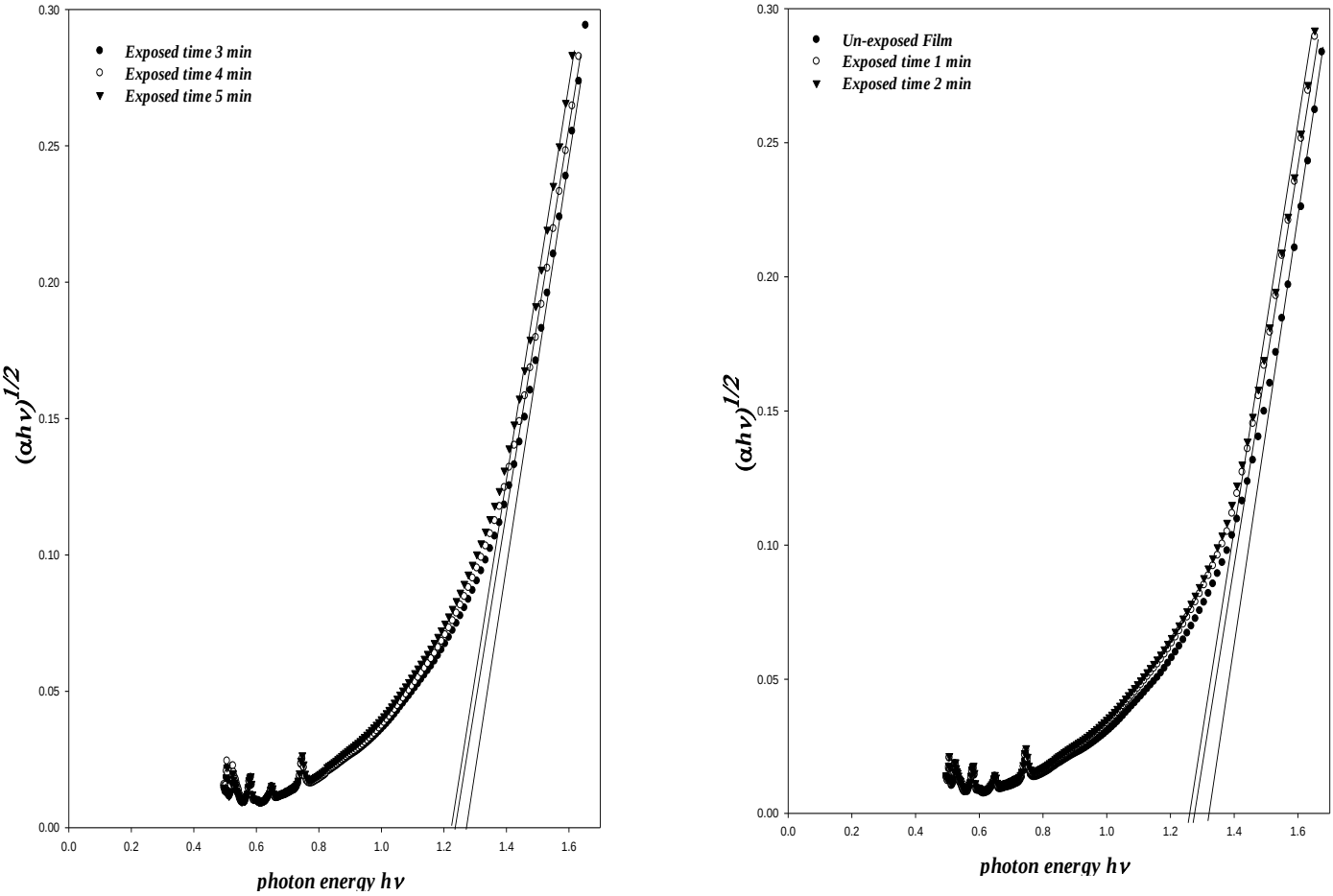


**Figure 6.** The optical absorption coefficient edge plotted as $(ah\upsilon)^{1/2}$ versus photon energy ($h\upsilon$) for un-irradiated and irradiated polyimide films with oxygen plasma exposure time.

**Table 4.** The optical band gap $E_g$ for PI as a function of plasma exposure time.

| Films | $\varepsilon_\infty$ | $\omega_p$ ($10^{12}$/s) | N/m* ($10^{17}$/cm$^3$) | Eg (eV) |
|---|---|---|---|---|
| Virgin Film | 1.836 | 9.831 | 6.911 | 1.328 |
| Exposed 1 min | 1.591 | 9.739 | 5.879 | 1.281 |
| Exposed 2 min | 1.512 | 9.691 | 5.534 | 1.266 |
| Exposed 3 min | 1.434 | 9.649 | 5.181 | 1.260 |
| Exposed 4 min | 1.351 | 9.639 | 4.890 | 1.241 |
| Exposed 5 min | 1.241 | 9.581 | 4.438 | 1.219 |

the confines of the constant conductivity model the equation 10 ($M_{-1}$ / $M_{-3}$) relates $E_d$ to the sum-rule moments $M_{-3}$ and $M_{-1}$. As a result, the dispersion energy may depend upon the detailed charge distribution within each unit cell, consequently, would then be closely related to chemical bonding may lie within a nearly localized orbital theory. Also, it was observed from Table 5 that $E_0$ was increased while $E_d$ was increased with the increasing plasma oxygen exposure time. Therefore, it is suggested that the observed in $E_d$ may be accounted for exposure sensitivity trend induced by increasing plasma oxygen exposure time.

## Conclusions

1) XRD obtained for virgin and polyimide films were exposure by oxygen plasma as confirmed by the semi

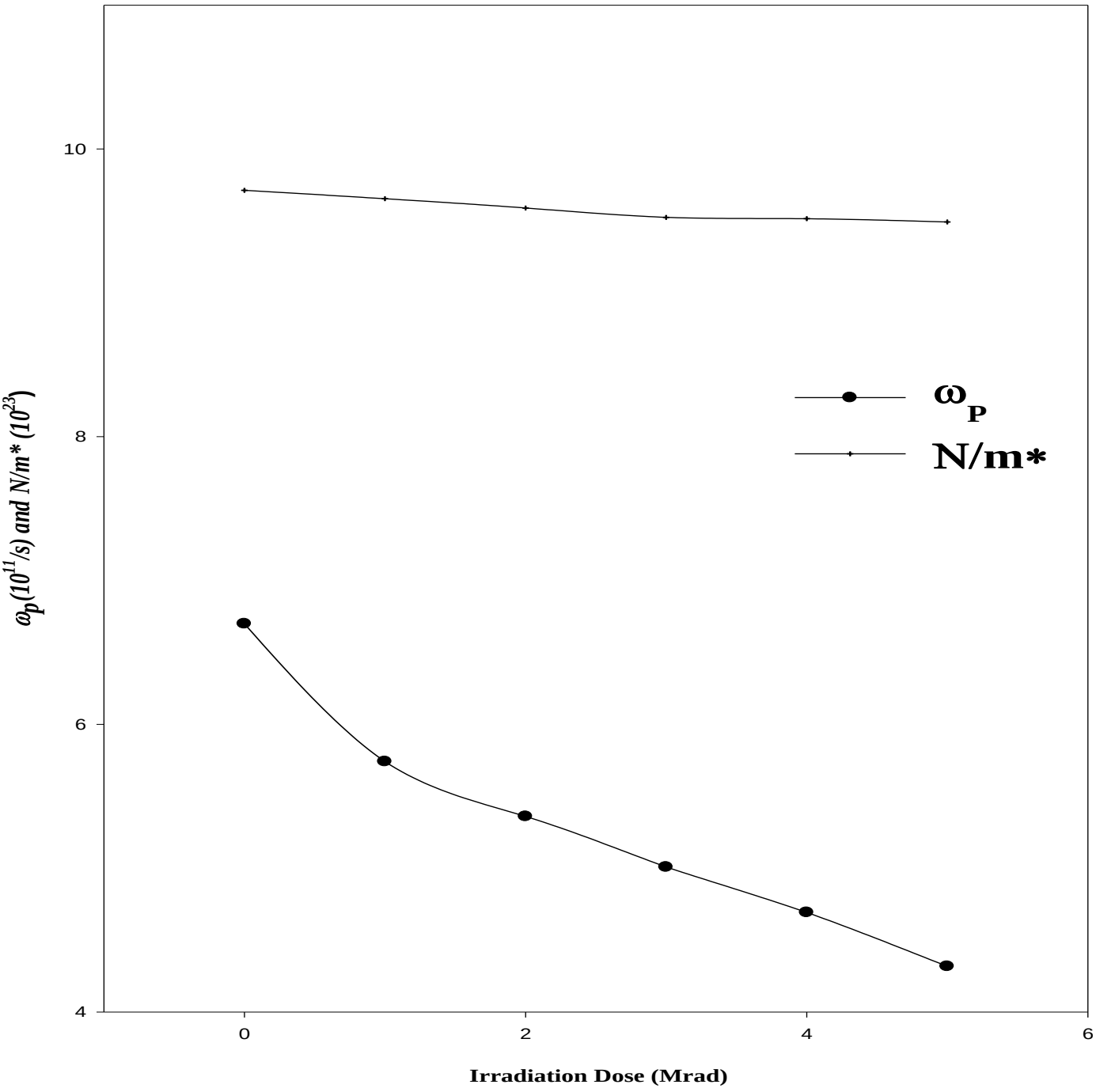


**Figure 7.** Variation of $\omega_p$ (plasma resonance frequency) with oxygen plasma exposure time for polyimide film.

crystalline nature for different films.

2) The intensity of these peaks for the exposed films is smallest than that of virgin film, indicating that the crystallinity becomes little obvious by increasing molecular weight.
3) The TGA curves of the virgin polyimide and exposure films at various time showed that the thermal stability increased with increasing time exposure.
4) Oxygen plasma exposure of polyimide films in the different time range 1 to 5 min has been investigated as a potential technique of refractive index modulating optical elements. There was an increase in the refractive index via increasing plasma exposure in the dispersion energy.
5) Single oscillator energies in the polyimide films were significantly influenced by Oxygen plasma effects. It was

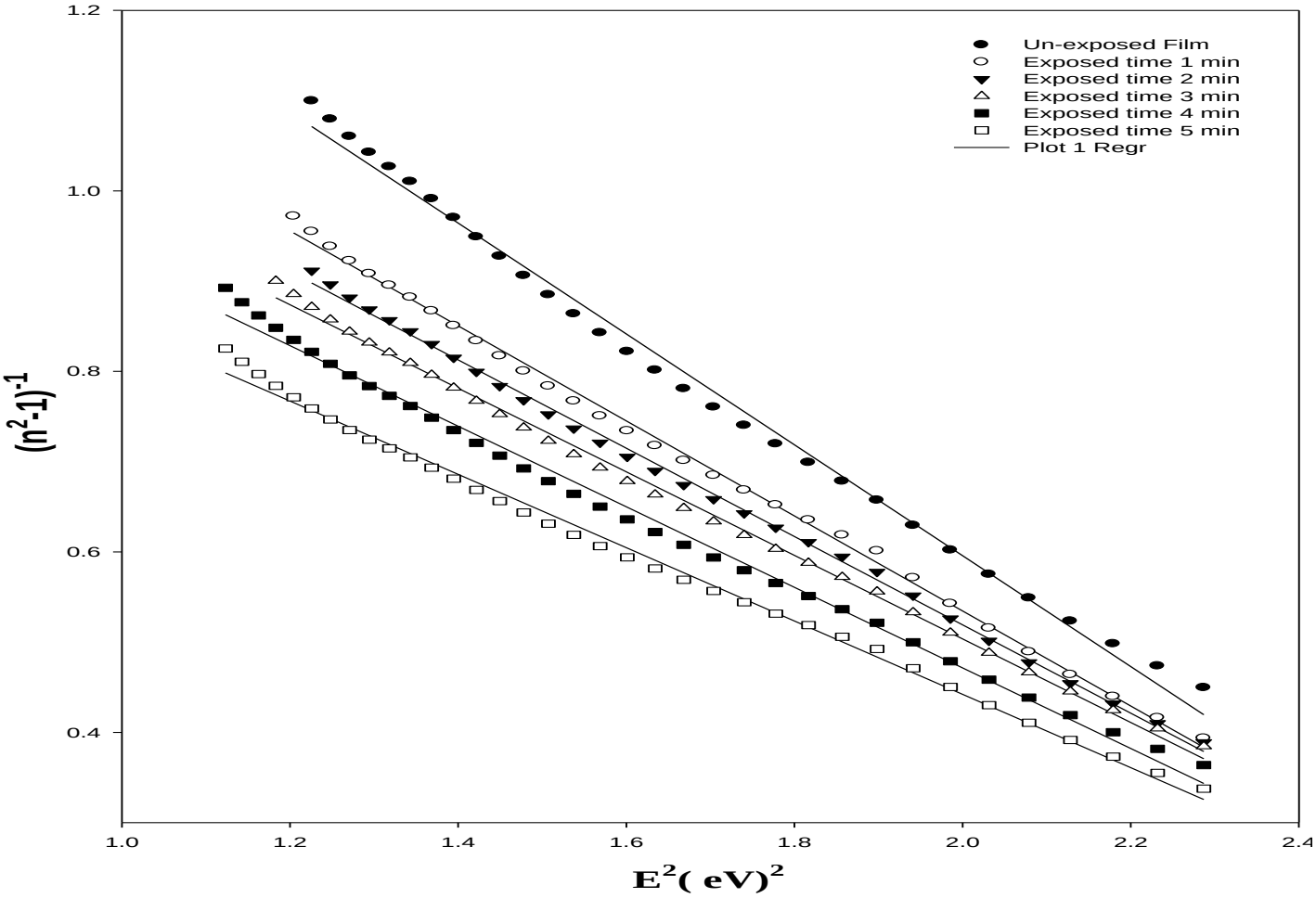


**Figure 8.** Plots $(n^2 - 1)^{-1}$ against square photon energy ($E^2$) with oxygen plasma exposure time for polyimide film.

**Table 5.** The single-oscillator energy and dispersive energy parameters for PI as a function of plasma exposure time.

| Films | $E_o$ | $E_d$ | $M_{-1}$ | $M_{-3}$ |
|---|---|---|---|---|
| Virgin Film | 1.723 | 0.945 | 0.548 | 0.185 |
| Exposed 1 min | 1.736 | 1.094 | 0.631 | 0.209 |
| Exposed 2 min | 1.750 | 1.168 | 0.668 | 0.218 |
| Exposed 3 min | 1.757 | 1.229 | 0.699 | 0.227 |
| Exposed 4 min | 1.758 | 1.274 | 0.725 | 0.235 |
| Exposed 5 min | 1.765 | 1.395 | 0.790 | 0.254 |

an increase in the dispersion energy and discussed in terms of the Wemple-DiDmenico model.

6) High frequency dielectric constant ($\varepsilon_\infty$) and N/m* ratio of free carrier concentration (N) to the free carrier effective mass (m*) are significantly affected by the change with increasing plasma exposure time.

7) The effect of Oxygen plasma exposure on the optical band gap obtained. Moreover, there was a decrease in the optical energy gap with increasing exposure time up to 5 min.

## ACKNOWLEDGEMENTS

The assistance provided by the "National Laboratory of Advanced Technology and Nano Science (INFM-TASC), Trieste, Italy" is highly appreciated and acknowledged. The authors wish to thank Simone Dal Zilio for this help

during working in the experimental Lab work.

## Conflict of Interest

The authors have not declared any conflict of interests.

### REFERENCES


Atta A (2013). Modification of the Surface Properties of Polyimide Films Using Oxygen Plasma Exposure. Arab J. Nucl. Sci. Appl. 46(5):115-123.

Atta A, Abdel Reheem AM, Abdel Rahman MM (2014).Effects of Argon plasma and ion beam on the morphology and wettability of polyethylene terephthalate (PET). J. Eng. Technol. Res. 6(2):18-26.

Atta A, Fawzy YHA, Bek A, Abdel-Hamid HM, Elokr MM (2013). Modulation of structure, morphology and wettability of PTFE surface by low energy ion beam irradiation. Nucl. Instr. Meth. Phys. Res B. 300:46–53.

Bin Ahmad M, Gharayebi Y , SapuanSalit M, Zobir Hussein M, Ebrahimiasl S, Dehzangi A (2012). Preparation, Characterization and Thermal Degradation of Polyimide (4-APS/BTDA)/$SiO_2$ Composite Films. Int. J. Mol. Sci. 13:4860-4872.

Gokan H, Esho S, Ohnishi Y (1982). Dry etch resistance of organic materials. J. Electrochem. Soc. 1:205.

Singh S, Kapoor A, Misra SCK, Tripathi KN (1996). Optimization of waveguide parameters of< i> bisphenol A</i> polycarbonate. Solid State Commun. 100:503-506

Hasegawa M, Horie K (2001). Photophysics, photochemistry, and optical properties of polyimides. Progress Polym. Sci. 26(2):259-335.

Jenkins FA, White HE (1985). Fundamental of Optics, McGraw-Hill, London: P. 479.

Kiryong H, John L (2002). Studies on the photodegradation of polarized UV-exposed PMDA–ODA polyimide films. J. Appl. Poly. Sci. 86:3072.

Kumar GA, Thomas J, George N, Kumar BA, Radhknshnam P, Nampoori VPN, Vallabham CPG (2000). Optical absorption studies of free (H2Pc) and rare earth (RePc) phthalocyanine doped borate glasses. Phys. Chem. Glass. 41:89.

Liu X, Yamanaka K, Jikei M, Kakimoto M (2000). Semicrystalline polyimides starting from AB-type monomers. Chem. Mater. 12:3885-3891.

Ma H, Jen AKY, Dalton LR (2002). Polymer-based optical waveguides: materials, processing, and devices. Adv. Mater. 14(19):1339-1365.

Kagami M, Ito H, Ichikawa T, Kato S, Matsuda M, Takahashi N (1995). Fabrication of large-core, high-Δ optical waveguides in polymers. Appl. Opt. 34(6):1041-6.

Mercanzini A,Colin P, Bensadoun JC, Bertsch A(2009). IEEE Trans. Biomed. Eng. 56(7):1909.

Qi K, Daoud WA, Xin JH, Mak CL, Tang W, Cheung WP(2006). Self cleaning Cotton. J. Mat. Sci. 16:4567-4574.

Saha NK, Joshi SV (2009).Performance evaluation of thin film composite polyamide nanofiltration membrane with variation in monomer type. J. Membrane Sci. 342:60–69.

Shalaby SE, Al-Balakocy NG, Abo El-Ola SM, Elshafei AM (2013). Effect of Surface Activation of Nylon-6 Fabrics by Plasma and Grafting With vinyl Monomers on Its Functional Finishing With $TiO_2$ Nanoparticles. J. Appl. Sci. Res. 9(3):1743-1753.

Soldera A, Monterrat E (2000). Mid-infrared optical properties of a polymer film: comparison between classical molecular simulations, spectrometry, and ellipsometry techniques. Polymer. 43:6027-6035.

Verdianz T, Simburger H, Liska R (2006). Surface modification of imide containing polymers I: Catalytic groups. Eur. Polym. 42(3):638-654.

Choi MC, Wakita J, Ha CS, Ando S (2009)."Highly transparent and refractive polyimides with controlled molecular structure by chlorine side groups". Macromolecules. 42 (14): 5112.

Wakkad MM, Shokr EKh, Mohamed SH, Wakkad MM (2000). Optical and calorimetric studies of Ge–Sb–Se glasses. J. Non- Crys. Solids . 265:157.

Wemple SH (1973). Refractive-index behavior of amorphous semiconductors and glasses. Phys. Rev. B7:3767.

Wemple SH, Didomenico M (1971). Behavior of the electronic dielectric constant in covalent and ionic materials. Phys. Rev. B3:1338-1351.

Yakuphanoglu F, Cukurovali A, Yilmaz I (2004). Determination and analysis of the dispersive optical constants of some organic thin films. Phys. B: Condensed Matt. 351:53-58.